The mass and radius of 5 FG-M binaries Discovered by SuperWASP

S. Gill[1], P.F.L. Maxted[1], B. Smalley[1], A. H. M. J. Triaud[2], A. von-Boetticher[2], L.Hebb[3], Y. Gomez-Chew Macqueo[4], B. Gary[5]

[1]Keele University, [2]University of Cambridge, [3]H & W. Smith Colleges, [4]Universidad Nacional Autonoma de Mexico, [5]Hereford Arizona Observatory

The role of FG-M binaries discovered by exoplanet surveys

There is a shortage of M dwarfs with well constrained mass and radius measurements. This is due to the relative faintness of double-lined eclipsing binaries and their low intrinsic brightness. Those that have been measured show that some are larger and hotter than models predict. It has been suggested that tidal interaction increase the interior magnetic field and inhibits convection resulting in an enlarged radius [1]. However, similar results have been seen with interferometric measurements of nearby M-dwarfs bringing into question whether spin-orbit interaction can be to blame [2].

FG-M binaries provide an opportunity to study M-dwarfs. They are discovered in abundance by the WASP survey and have quality RV measurements as part of exoplanet candidate follow-up observations. These systems are single-lined eclipsing binaries so stellar models are needed to estimate the mass of the primary star. The mass of the secondary can then be estimated when combined with an orbital fit. There is an ongoing project [3-5] to measure the mass and radius of transiting FG-M systems discovered by the WASP survey (Fig. 1). These measurements will help test stellar models and provide reliable points from which to derive empirical relations for the bottom-end of the main sequence. The recent revelations of the TRAPPIST-1 system and Proxima Centauri A have captured the attention of scientist and public alike, meaning it is ever more relevant to study low-mass stars. We have obtained follow-up photmetry for 5 FG-M binaries discovered by the WASP survey and we present their mass and radius in context of evolutionary models and recent measurements.

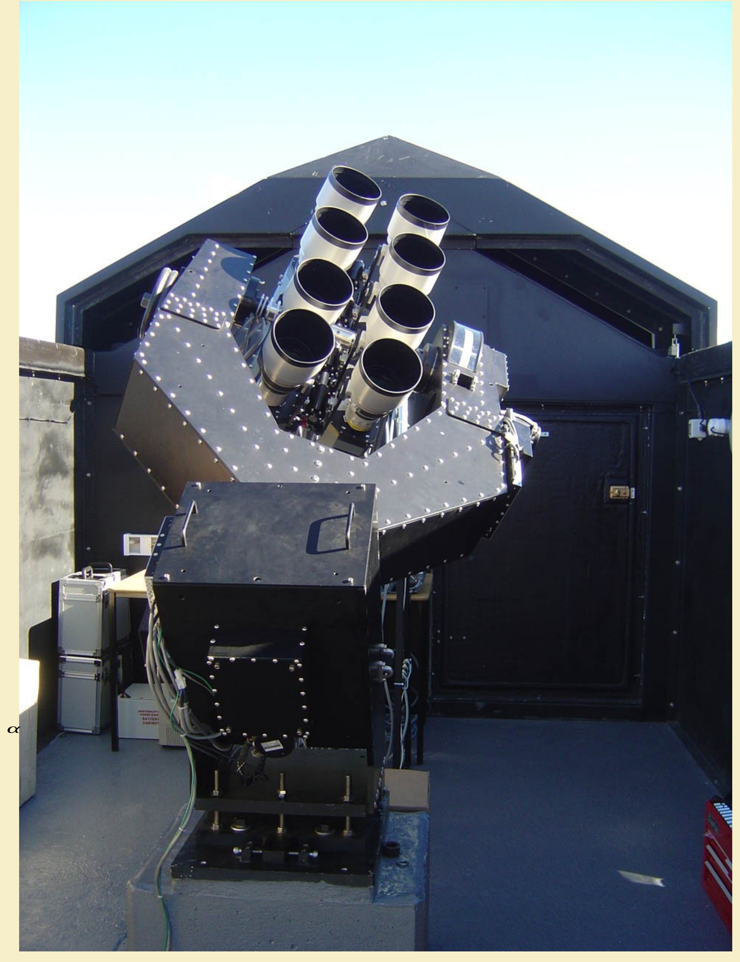

Fig. 1 SuperWASP-South, located at Sutherland, South Africa, consists of 8 cameras monitoring the brightest souther targets in search of transit signatures mimicking large, gaseous exoplanets.

Data acquisition

All 5 systems have light curves from SuperWASP from either the norther site in La Palma (Spain) or the south site in Sutherland (South Africa). As part of the exoplanet candidate follow-up, we obtained spectroscopic orbits with the CORALIE echelle spectrograph. For the only northen target, J1847+39, we used observations from the spectrograph on the Issac Newton telescope (R~5000) at the Roque de los Muchachos observatory. Follow-up photometry was required to measure the mass and radius to the desired precision of a few percents. We used the 1-m telescope at the South African Astronomical Observatory to obtain follow-up transit observations for three targets (J2349-32 [I], J2308-46 [R] & J1436-13 [R]). For J0218-31 we observed a single transit with the SMARTS telescope at the Cerro Tololo Inter-American Observatory in g', r', i' & z' pass bands simulatenously. For J1847+39, we used multiple transits observed in different pass bands (clear blue-blocking, z' & g') from the 14" Meade telescope in dome 2 of the Hereford Arizona Observatory, America.

Atmospheric parameters

There are two crucial parameters required to accurately estimate the mass of the FG star: effective temperature and [Fe/H]. These are best estimated from the co added spectrum obtained from radial velocity measurements. For targets with CORALIE spectra, we found that even co added spectra had a relatively low signal-to-noise (S/N). To circumvent this, we decided to use wavelet analysis [6] which compares a discrete subset of wavelet coefficients to those from a grid of models to estimate atmospheric parameters1. This allowed us to exclude noisy artefacts and relax normalisation constraints which would otherwise hamper spectral fitting.

For EBLM J1847+39, we obtained INT spectra which is limited to the region around H-alpha and is not suited to wavelet analysis. Instead, we fit the wings of the H-alpha line to estimate effective temperature and fit a small number of Fe lines to constrain [Fe/H]. Fo all targets, we fitted photometry from 2MASS, APASS9 and SDSS to validate estimates of effective temperature and estimate E(B-V).

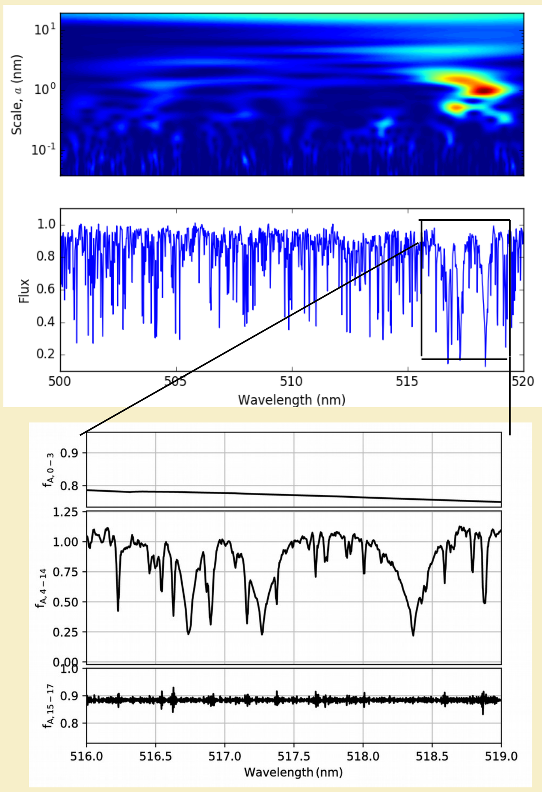

Fig. 2 (top-upper) The power spectrum of a discrete wavelet decomposition for of a small section of the CORALIE spectrum of WASP-19 around the Mg triplets (top-lower). We also show the wavelet reconstruction of different subsets of coefficients which correspond to low-order continuum trends (lower-top), high-order noise (lower-bottom) and a wavelet filtered spectrum.

Orbital fit

We fitted the SuperWASP photometry to gain initial estimates for transit parameters and to provide updated epoch times. The follow-up photometry was fitted simultaneously with the radial velocity measurements with a Monte Carlo sampler. We use the parallel stretch move algorithm implemented with the python package emcee. Our fitting routine is similar to that of [3] with two extra free parameters: a period drift, P_dot, and a systematic velocity drift (Vdot). We initialised 50 walkers and generated 100,000 draws from each chain. The first 50,000 draws were considered to be in the burn-in phase and discarded. The model parameters with the highest likelihood were accepted with uncertainty from the standard deviation of models.

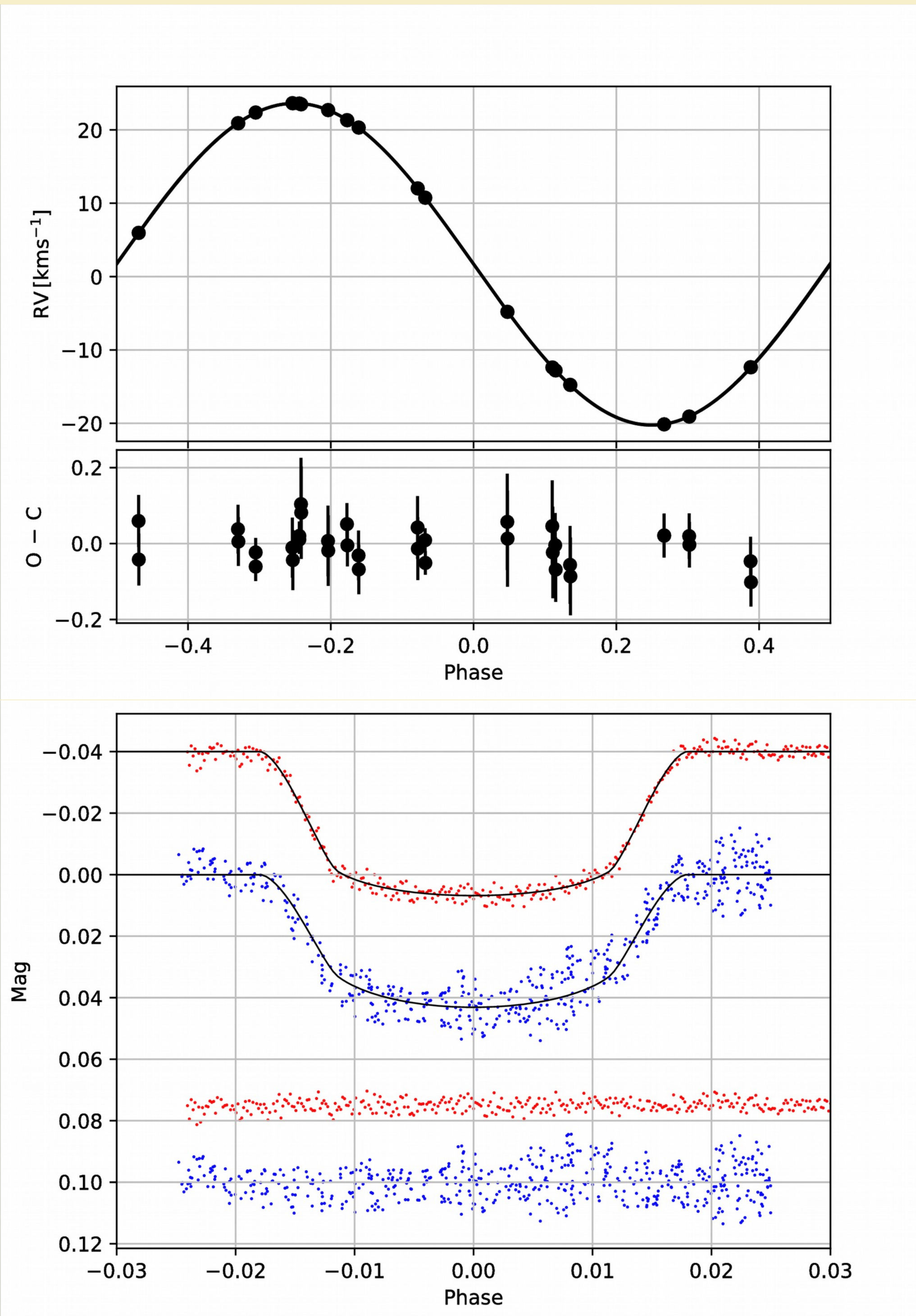

Fig. 3 (top) the radial velocity measurements along with the best fitting model for EBLM J2349-32. (bottom) The best fitting transit model for R-band photometry obtained from SAAO's 1-m telescope (red) and the same model for SuperWASP photometry (blue).

Estimating mass and radius

We use a modified version of BAGEMASS [7] to interpolate the best fitting stellar models and estimate the mass of both components in each system. This version uses age, [Fe/H]i, M1, M2 and fwhm as jump parameters with the mass function, f(m), Teff, *, Log L*, [Fe/H]s and R*/a from the orbital fit as input parameters. We use the same GARSTEC evolutionary models provided with BAGEMASS. We generate a single walker and generate 50,000 draws after an initial bur- in phase of 50,000 draws. The model with the highest likelihood is accepted with uncertainty equal to the standard deviation of models (Fig. 4).

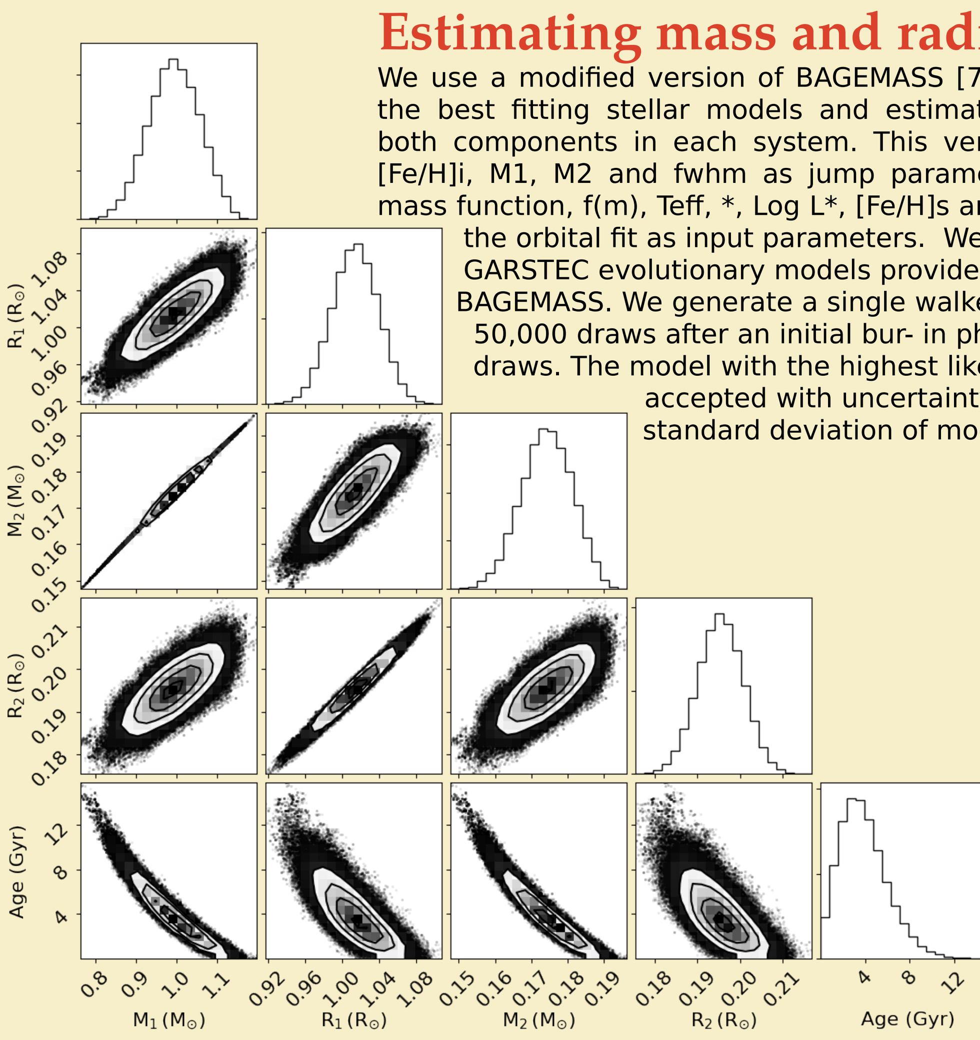

Fig. 4 Corner plot displaying the posterior probability distributions for the mass, radius and age of both components in EBLM J2349-32.

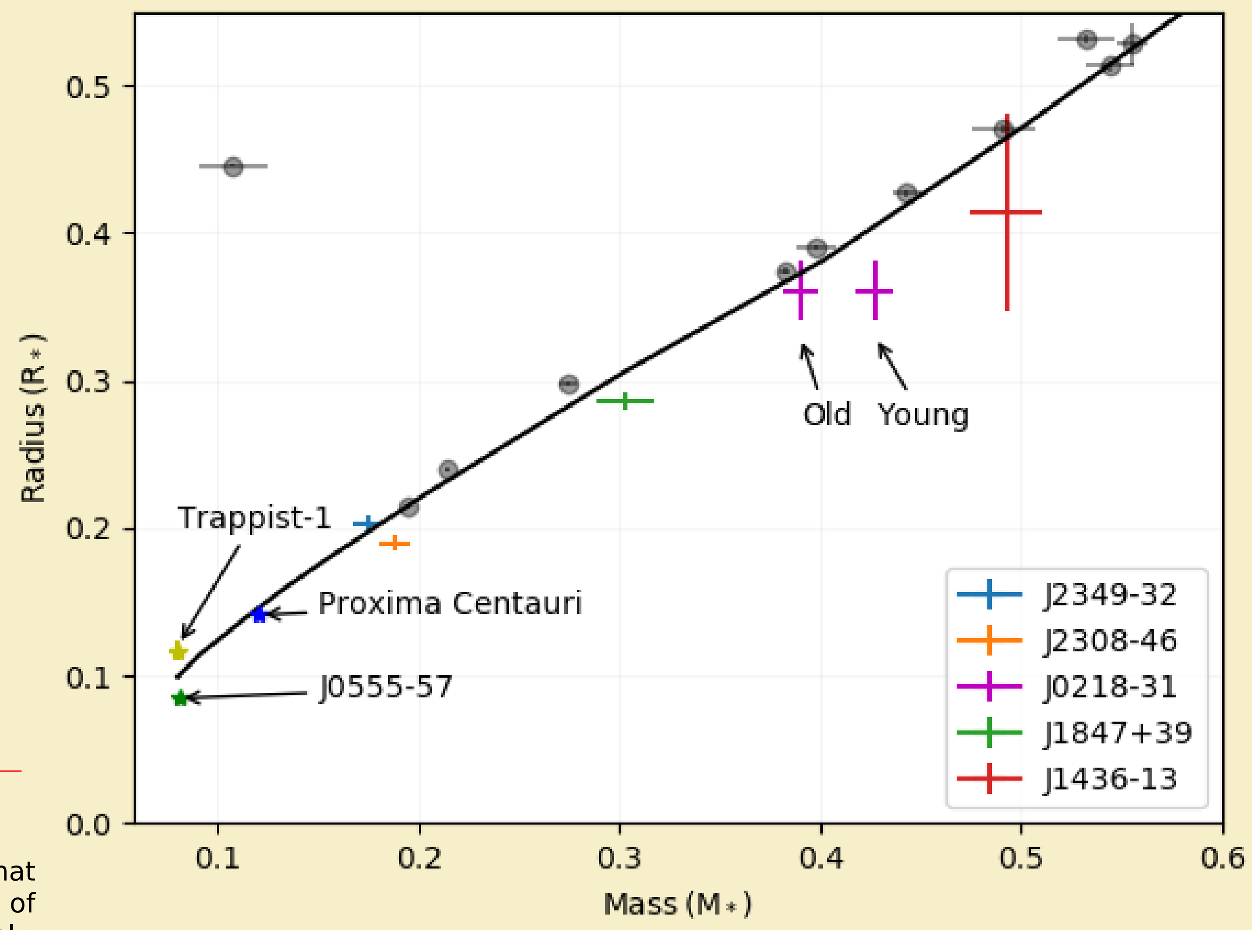

Fig. 5 The mass radius diagram for 5 EBLMS along with EBLM J0555-57, Proxima Centauri, Trappist-1 and a selection of low-mass companions (black) from DEBCAT (Southworth 2015). The 3 Gyr isochrone for solar metalicity is also plotted [8].

Discussion

EBLM J2349-32

The best fitting orbital solution to our 20 radial velocity measurements shows that the orbital eccentricity is small (e<0.01). The follow-up light curve in I band is of exceptional quality enabling us to tie down the size of both components precisely. The solution from EBLMMASS describes a low mass M-dwarf that is slightly inflated compared to solar-metalicity models from Barraffe 2015.

EBLM J2308-46

The SuperWASP photometry displays moderate ellipsoidal variation (~0.01 mag) suggesting one or more of the stars are best described with Roche geometry. To obtain a better fitting epoch, we fit SuperWASP photometry with a Roche model and fix the gravity darkening coefficient to 0.1 to describe the ellipsoidal variations. The follow-up R band photometry from the SAAO 1-m telescope was not fit with Roche models since we detrended the single SAAO transit with a 4th order polynomial using chosen continuum regions. The best models from EBLMMASS suggest a slightly evolved primary and a relatively dense M-dwarf which could probably be explained by the low-metalicity of the system ([Fe/H] = -0.15).

EBLM J0218-31

We obtained 98 RV measurements, of which 28 covered the Rossiter McLaughlin effect. The best orbital fit suggests an aligned (λ= 4 ± 7°), circularised orbit. When combined with [Fe/H], T_{eff} in BAGEMASS we find that the primary star lies on around the post-main sequence blue hook (Henyey hook) where hydrogen is low enough for fusion to effectively stop, and the star contracts and heats up (Fig. 6). Unfortunately this creates some ambiguity in our mass estimate for the primary (and thus the M-dwarf companion) resulting in two near-equal solutions. We plot them both in Fig. 5.

EBLM J1847+39

Spectra for this northern target were obtained using the IDS spectrograph on the 2.5-m INT. The spectra cover the region around the H-alpha line and have a resolution R~10,000. Wavelet analysis is not suitable over a short wavelet range, so we instead use H-alpha fitting to measure T_{eff}, confirmed with photometric fitting from 2MASS, NOMAD, and ASPASS9. There are only a few iron lines in the INT spectra which were fitted with the synthesis method to obtain an estimate for [Fe/H] with a precision lower that the other targets in our sample. We fitted RVs with a single transit observed from HAO (CBB, g' and z') to reveal an eccentric orbit (e ~ 0.21). The best fitting solution from BAGEMASS is a 0.3 M_{sol} M-dwarf which is slightly denser than predicted.

EBLM J1436-13

Our analysis of 13 co-added CORALIE spectra show that the primary star shows moderately fast rotation (Vsini ~ 18 kms^{-1}) and is slightly metal poor ([Fe/H] ~ -0.1). The single R-band transit obtained from the SAAO 1-m telescope is V shaped with a fitted impact parameter of b = 0.92 ± 0.07. This results in the radius of both components being poorly constrained. The best fitting solution from BAGEMASS reveals the highest M-dwarf mass in our sample (0.49 ± 0.02 M_{sun}), with a radius 17% below BHAC15 models [8].

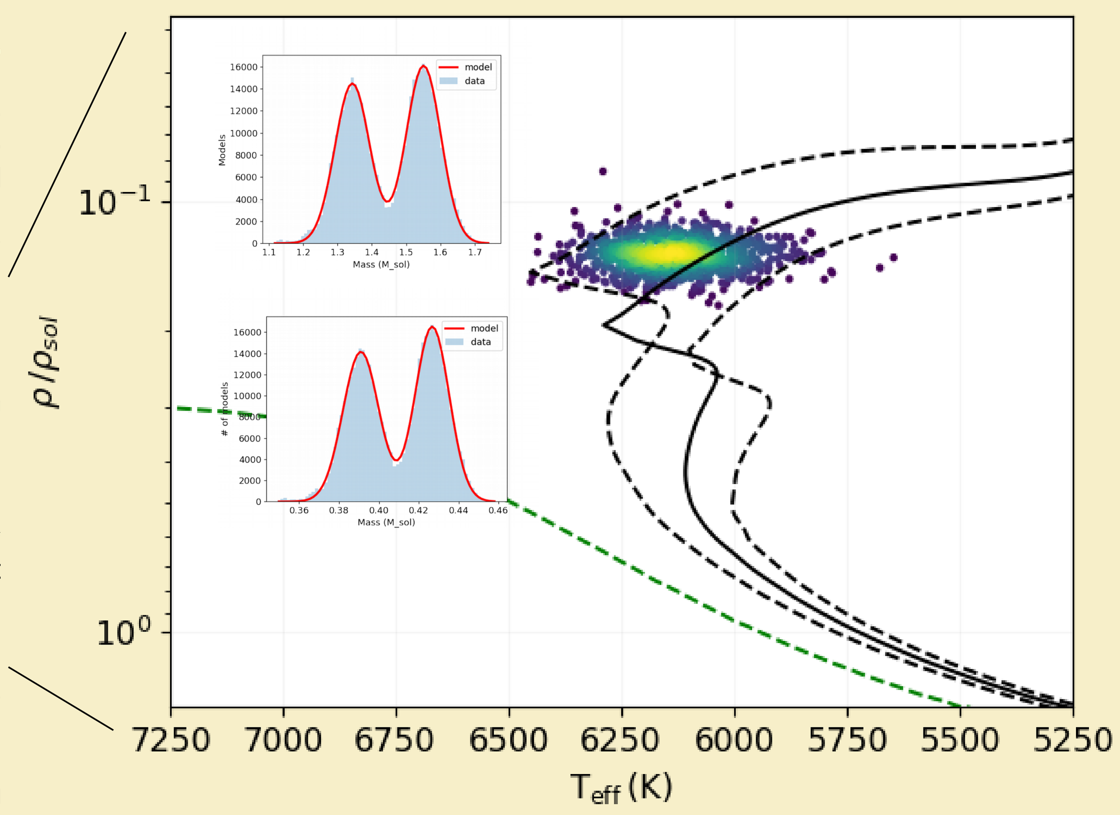

Fig. 6 The location of EBLM J0218-31A on a density-temperature diagram and the resulting posterior probability distributions for the mass of the primary (top) and the M dwarf (bottom).

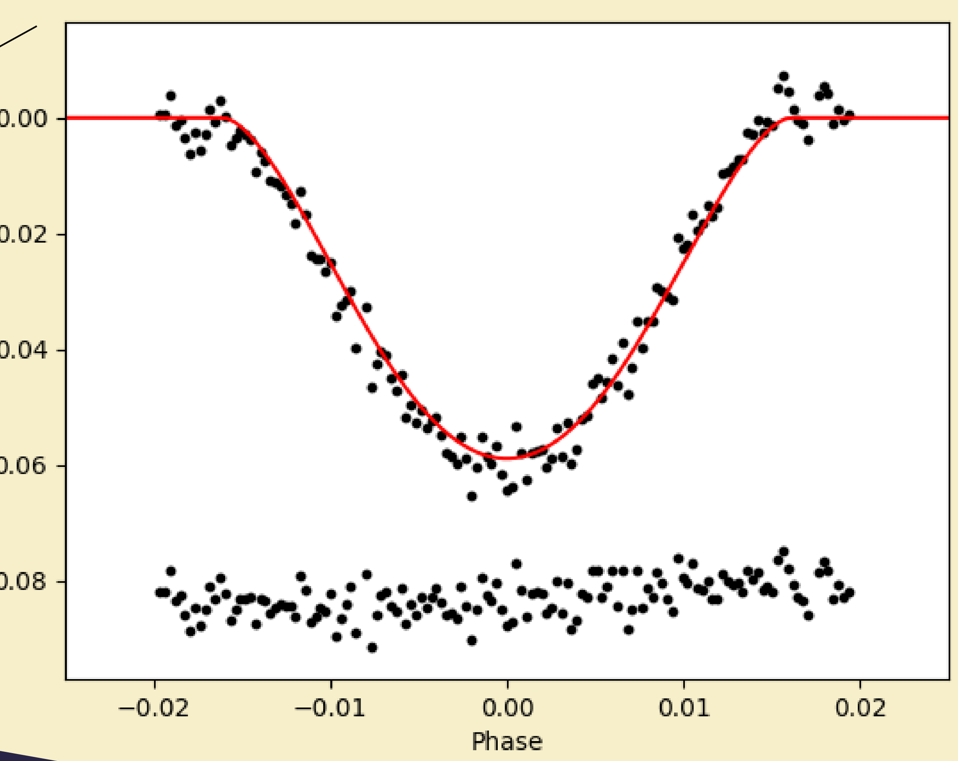

Fig. 7 A single transit in R band for EBLM J1436-13 observed with the 1-m telescope, SAAO, plotted alongside the best fitting model (red). The transit is V-shaped resulting in a degeneracy between R_1 and *b*.

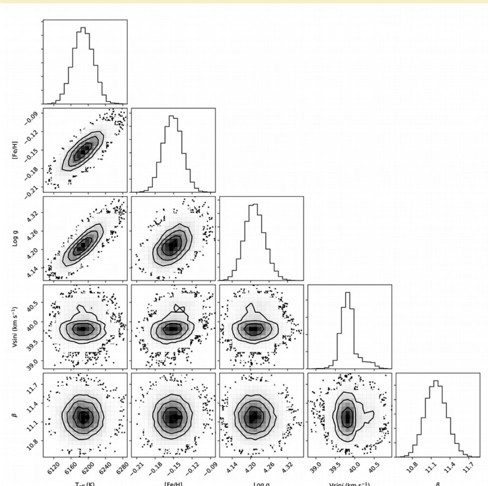

We have implemented the wavelet analysis of echelle spectra into a python module *waveletspec* which is available for the community to use. (https://github.com/samgill844/waveletspec)

Third light from transiting M-dwarfs

M-dwarfs in binary systems emit light and so a simple transit model with a non-emitting transiting body may not be applicable. To test this, we take the 3 Gyr isochrones [8] to estimate the luminosity of each component in EBLM J1436-13 (q ~ 0.41). We find that the M-dwarf contributes 1.2% of the total flux. This is a small contribution, but will inevitably cause a shallower transit depth and a mis-measured radius. To test this, re-fit J1436-13 with a fixed third light contribution of 1.2% and find that the radius of the primary decreased by 0.04 R_{sun} and the secondary by 0.01 R_{sun}. This is a 1% decrease in the radius of the M-dwarf which emphasizes the need to account for third light when the mass fraction approaches unity. For our lowest mass-fraction (J2308-46, q ~ 0.15), we find the third light contribution to have an effect below the uncertainty we can measure the stellar radius.

Helium abundance and mixing length

For this analysis, we fixed the mixing length parameter to 1.78 and the initial helium abundance to 0.26646 with null enrichment. The uncertainty of mixing length parameter and helium abundance can propagate through to estimates of mass and age. From Table 4 of Maxted et al. 2014 of six solar-type stars we find that uncertainty in age can be as much as 1 Gyr for helium abundance and 1.85 Gyr for mixing length parameter by changing each parameter by their respective uncertainty (ΔY = 0.02, $\Delta\alpha_{mlt}$ = 0.2). Similarly for mass, we find that helium abundance can introduce and uncertainty 0.04 M_{sun} and an uncertainty from the mixing length parameter of 0.03 M_{sun}. Added in quadrature, we find typical uncertainties of 0.05 M_{sun} from uncertainties in mixing length and helium abundance, which is comparable to uncertainties from EBLMMASS.

Future work

In this work we demonstrate a tool set to measure the mass, radius and age of M-dwarfs in binary systems with solar type stars. The EBLM project will measure hundreds of FG-M binaries in order to empirically calibrate the mass-radius-composition-luminosity relations at the bottom end of the main sequence. Such calibrations will improve our understanding of exoplanets around low-mass stars which have recently captured the interest of scientists and public alike.

The WASP project has discovered hundreds of EBLMs similar to those in this sample. Many of these have high precision radial velocity measurements, but the quality of SuperWASP photmetry is not good enough to measure the radius to the desired precision of a few percents. We will continue to obtain follow-up transit photometry for as many EBLMs as possible. We already have K2 light curves for 3 EBLM systems, which will allow us to measure transit parameters to high precision, and model spot distributions and oscillations if present.

References

[1] Morales J. C., et al., 2010, ApJ, 718, 502
[2] Spada F., et al ., 2013, ApJ, 776, 87
[3] Triaud A. H. M. J., et al., 2013, A&A, 549, A18
[4] Gomez Maqueo Chew, Y., et al., 2014, A&A, 572, A50
[5] Von Boetticher, A., et al., 2017, 1706.08781
[6] Gill, S., et al., 2017, in prep
[7] Maxted, P. F. L., et al., 2015, A&A, 575, A36
[8] Baraffe, I., et al., 2015, A&A, 577, 42B
[9] Southworth, J., 2015, ASPC, 496, 164S